Enzyme and Microbial Technology 161 (2022) 110114

Contents lists available at ScienceDirect

Enzyme and Microbial Technology

journal homepage: www.elsevier.com/locate/enzmictec

Co-expression of an isopropanol synthetic operon and eGFP to monitor the robustness of *Cupriavidus necator* during isopropanol production

Catherine Boy, Julie Lesage, Sandrine Alfenore, Stéphane E. Guillouet, Nathalie Gorret *

TBI, Université de Toulouse, CNRS, INRA, INSA, Toulouse, France

ARTICLE INFO

Keywords:
Cupriavidus necator
eGFP
Isopropanol
Fed-batch cultivations
Flow cytometry
Plasmid expression levels
Single cells

ABSTRACT

Phenotypic heterogeneity in bioprocesses is suspected to reduce performances, even in case of monoclonal cultures. Here, robustness of an engineered isopropanol-overproducing strain and heterogeneity of its plasmid expression level were evaluated in fed-batch cultures. Previously, eGFP was identified as a promising plasmid expression reporter for *C. necator*. Here, the behavior of 3 engineered strains (isopropanol overproducer, eGFP producer, and isopropanol/eGFP co-producers) was compared at the single-cell and population levels. Production yields and rates have been shown to be dependent on isopropanol/acetone tolerance. A link could be established between the variations in the fluorescence intensity distribution and isopropanol/acetone production using the eGFP-biosensor. Co-production of isopropanol and eGFP exhibited cumulative metabolic burden compared to single overexpression (isopropanol or eGFP). Expression of eGFP during isopropanol production resulted in lower isopropanol tolerance with a loss of membrane integrity resulting in protein leakage and reduced plasmid expression. The co-expression of heterologous isopropanol pathway and eGFP-biosensor enabled to demonstrate the heterogeneity of robustness and plasmid expression at the single cell level of *C. necator*. It highlighted the conflicting interactions between isopropanol overproduction and eGFP reporter system. Fluorescent reporter strains, a crucial tool for monitoring subpopulation heterogeneity although biases have to be considered.

1. Introduction

Phenotypic heterogeneity occurs when a clonal population exhibits several distinct phenotypes even in homogeneous environments. Even monoclonal cultures grown in homogeneous environments can experience cellular heterogeneity. Thus, the amount of protein produced from a particular gene will vary among cells in a population and also over time for a single cell. Most of the time, this is due to heterogeneous gene expression [1–5]. Noise in gene expression is a natural phenomenon arising in two ways: “intrinsic” and “extrinsic” noises [6–8].

In engineered strains, the insertion of heterologous genes is an additional source of cell-to-cell variability. Indeed, the maintenance and expression of these heterologous genes induce a metabolic load on the host cells. In most cases, the metabolic load is due to the consumption of extracellular transcriptional resources during the expression of recombinant genes [9]. Therefore, two biological phenomena are in competition within the engineered strains: the maintenance of the recombinant genes and the growth of the host cell [10]. Resource redistribution could significantly disrupt translation, especially if mRNAs expressed from the heterologous gene sequence encode strong RBS (*i.e.* Ribosome Binding Sites). In this case, a significant proportion of ribosomes should no longer be available for expression of host genes. Metabolic load leads to decreased growth rate and overall physiological changes. Therefore, the performance of engineered microorganisms toward the production of the recombinant molecules of interest decreases. Finally, the production of a recombinant molecule might be toxic for host cells, which might eventually cause plasmid expression loss [9].

Whether due to stochastic gene expression or metabolic load, population heterogeneity is thought to decrease production yields and enhance process instability. Thus, securing phenotypic homogeneity in engineered microbial populations is of major interest for synthetic biology and bioprocess optimization [11–13]. Bioprocesses are traditionally evaluated from measurements based on mean values of cell populations. However, such methods are not suitable to study the behavior of individual cells especially within heterogeneous cell populations. Single-cell techniques have been intensively investigated in recent years to trigger key biological mechanisms in living single cells, such as stochasticity of gene expression [14–21]. A wide variety of

* Correspondence to: TBI, Université de Toulouse, CNRS, INRA, INSA, 135 Avenue de Rangueil, 31077 Toulouse Cedex 04, France.
E-mail address: ngorret@insa-toulouse.fr (N. Gorret).

https://doi.org/10.1016/j.enzmictec.2022.110114
Received 11 March 2022; Received in revised form 19 July 2022; Accepted 16 August 2022
Available online 19 August 2022

proteins have been studied as gene expression reporters. Among them the most used are: *lacZ* encoding the *E. coli* beta-galactosidase, *luxAB* encoding the *Vibrio harveyi* luciferase and *gfp* encoding the green fluorescent protein from *Aequorea victoria* [2]. GFP reporter proteins have often been coupled to flow cytometry. Nowadays, gene reporters based on GFP and its derivatives are the most widely used biological tools for dynamic analysis of gene expression in living cells [14,22–27].

C. necator H16 has a versatile metabolism and is naturally able to consume both organic [28–31] and inorganic carbon sources [32–35]. *C. necator* is able to store up to 80 % of its dry cell weight in poly--β-hydroxybutyrate (*abbr.* PHB) [36,37], by diverting carbon flow at the acetyl-coA node toward PHB biosynthesis under conditions of nutrient limitation and excess carbon [38]. By the way, *C. necator* has been engineered to produce acetyl-coA derived compounds: isopropanol [32, 35,39,40], isobutanol [41], alka(e)ne [34], carboxylic acids [42,43], alpha-humulene [44] and methyl ketones [45], both heterotrophically and autotrophically.

In the present work, the heterologous production of isopropanol by *C. necator* Re2133 was chosen as a case study to assess plasmid expression levels during production of an unnatural potentially toxic product. The production titers achieved by such engineered strains could be limited by alcohol toxicity in host strains [46]. The high hydrophobicity of solvent increases its toxic impact on host cells, in effect leading to solvent accumulation in the cytoplasmic membrane causing various side effects [47–49]. Solvents can also denature biological molecules and lead to protein unfolding, DNA and lipid damage, RNA unfolding or degradation [49], consequently, growth inhibition or cell death. Expression of *groESL* in solvent-producing microorganisms has been shown to increase cell tolerance [47]. Marc et *al.* (2017) showed that *groESL* genes over-expression led to a better tolerance to exogenous isopropanol and to a lower cell permeabilization toward higher isopropanol concentrations during fedbatch culture.

Previously we designed and validated an eGFP-based plasmid expression level monitoring system for *C. necator* [15,20,21]. Here, the eGFP was expressed under the constitutive promoter P_{lac} in order to monitor the level of plasmid expression and inserted into the plasmid pEG7c containing an inducible isopropanol synthetic operon [40]. The use of an inducible promoter has been shown to achieve better isopropanol production performance because it allows growth and production to be uncoupled to help the cell cope with the inhibitory effect of isopropanol. The overall objective of this work was to study the impact of the production of a toxic recombinant molecule on the levels of plasmid expression. The present study was supported by macroscopic data (metabolite concentrations, production/consumption yields and rates) as well as single-cell analysis (flow cytometry).

2. Material and methods

2.1. Strain, plasmids and media

2.1.1. Strains

C. necator Re2133 [28] was used as an expression strain. This strain was obtained by deletion of the genes coding for acetoacetyl-CoA reductases (*phaB1B2B3*) and for PHA synthase (*phaC1*) from the wildtype strain *C. necator* H16/ATCC17699 which was resistant to gentamicin (Gen^R). The strains *Escherichia coli* S17–1 and Top10 were used during plasmid construction.

2.1.2. Plasmids

The plasmids pEG7c (arabinose induced isopropanol operon), pCB1 (constitutive Plac-eGFP) and pJLCB2 (combining the two genetic parts) were used in this work (Table 1). The plasmid maps are provided in Supplementary Material 1. The design and associated molecular biology protocols for the construction of these plasmids were explained in more details in [21,32,40].

Table 1
Plasmids used in this work.

Strains	Relevant characteristics	References
Re2133	*Cupriavidus necator* H16 Δ*phaB*$_1$*B*$_2$*B*$_3$*C*$_1$ (Gen^R)	[55]
Plasmids		
pBBAD	pBBR1MCS-2 derivative (Kan^R), P_{Bad} (L-Arabinose inducible promoter)	[56]
pEG7c	pBBad (Kan^R), isopropanol operon *phaA* – RBS – *ctfAB* – RBS – *adc* – RBS - *adh* inserted into the multiple cloning site (MCS), P_{Bad}	[40]
pCB1	pBBad (Kan^R), P_{lac}-*egfp*	[15]
pJLCB2	pEG7c (Kan^R), P_{lac}-*egfp* (on the opposite strand, compared to pCB1)	[32]; This work

2.1.3. Media

The rich medium for precultures was composed of 27.5 g l^{-1} Tryptic Soy Broth (TSB, Becton Dickinson, Sparks, MD, USA) with addition of 10 mg l^{-1} gentamicin and 200 mg l^{-1} kanamycin as final concentration. For Tryptic Soy Agar (*abbr.* TSA) plates, 20 g l^{-1} agar was added to the TSB medium.

For molecular biology, the rich Lysogeny broth medium (*abbr.* LB) was used and composed of 10 g l^{-1} of peptone, 5 g l^{-1} of yeast extract and 10 g l^{-1} of NaCl. For LB agar plates, 20 g l^{-1} agar was added to the LB medium.

The mineral medium used for flasks cultivation was previously described in Lu et *al.* [50]. Gentamicin (10 mg l^{-1}) and kanamycin (200 mg l^{-1}) were added to this medium. Fructose (20 g l^{-1}) and NH_4Cl (0.5 g l^{-1}) were respectively used as carbon and nitrogen sources. The mineral medium used for bioreactor cultivation was composed as follows (per liter): $(NH_4)_2SO_4$, 2.8 g; $MgSO_4$ * 7 H_2O, 0.75 g; phosphorus (Na_2HPO_4 *12 H_2O, 1.5 g; KH_2PO_4, 0.25 g); nitrilotriacetic acid, 0.285 g; ammonium iron(III) citrate (28 %), 0.09 g; $CaCl_2$, 0.015 g; trace elements (H_3BO_3, 0.45 mg; $CoCl_2$ *6 H_2O, 0.3 mg; $ZnSO_4$ *7 H_2O, 0.15 mg; $MnCl_2$ *4 H_2O, 0.045 mg; Na_2MoO4 *2 H_2O, 0.045 mg; $NiCl_2$ *6 H_2O, 0.03 mg; $CuSO_4$, 0.015 mg). Fructose was used as sole carbon source with an initial concentration of 30 g l^{-1}. No antibiotics (*i.e.* gentamicin and kanamycin) were added in bioreactor cultures in order to evaluate plasmid stability without selection pressure.

2.2. Fed-batch cultivations on fructose

Precultures and batch phases were performed according to the protocol detailed in [15] to avoid any cell growth limitation. The fed-batch phases were initiated when nitrogen depletion was reached in the mineral medium (corresponding to 4 $g_{CDW}{\cdot}l^{-1}$ biomass). Nitrogen (using ammonium,) was the limiting substrate and was fed in the bioreactor by a calibrated peristaltic pump with an exponential flow rate set at 0.04 h^{-1}. This growth rate was chosen based on previous works to investigate isopropanol producing conditions. The initial fructose concentration was 30 g l^{-1}. After the start of the fed-batch phase, when the fructose concentration reached 20 g l^{-1}, fructose was fed exponentially in the bioreactor to maintain a constant residual concentration of 20 g l^{-1}. Two guard flasks, kept in ice, allowed the re-solubilization of the gaseous fractions of acetone and isopropanol in order to quantify their total production both in the liquid phase and gaseous phase.

To prevent nutrient limitation, a phosphorus solution (7 $ml{\cdot}l^{-1}$) and a trace element solution (2 $ml{\cdot}l^{-1}$) were added for every 10 $g_{CDW}{\cdot}l^{-1}$ of biomass produced.

2.3. Analytical procedure

2.3.1. Biomass characterization

Biomass quantification was achieved through optical density (600 nm) and cell dry weight measurements. These techniques were described in [15].

2.3.2. Metabolite quantification

Cells samples were centrifuged, and supernatants were filtrated (0.2 μm PTFE syringe filters, VWR) before being used for substrate and products determination. The residual fructose and organic acids concentrations were quantified by high-performance liquid chromatography (HPLC). The HPLC instrument (Series 1100, Agilent) was equipped with an ion-exchange column (Aminex HPX-87H, 300 ×7.8 mm, Bio-Rad, Hercules, CA, USA) protected with a guard column (Cation H+ cartridge, 30 × 4.6 mm, Bio-Rad) and coupled to a RI detector and an UV detector (λ = 210 nm). The column was eluted with 2.5 mM H_2SO_4 as a mobile phase at 50 °C at a flow rate of 0.5 ml·min^{-1}. Residual nitrogen was quantified by higher-pressure ionic chromatography (HPIC). The HPIC instrument (ICS-2100 RFIC, Dionex) was equipped with an IonPac™ CS16 column (RFIC™, 3x50mm, BioRad) and an ion suppressor CERS 500 (2 mm, Thermo Scientific). The column was eluted with 30 mM metanesulfonic acid as a mobile phase at 40 °C and a 40 mA ion suppressor current, at a flow rate of 0.36 ml·min^{-1}. Isopropanol and acetone concentrations were also determined by gas chromatography (GC), with a GC system 6890 A Series (Hewlett Packard®, USA) and a column SupelQ-Plot 30 × 0.53 mm (ID). Internal standard was 1 g l^{-1} propionic acid.

2.3.3. Plate count

Plasmid stability was quantified by parallel plate count on antibiotic selective TSB Petri dishes (10 mg l^{-1} gentamicin and 10 mg l^{-1} gentamicin + 200 mg l^{-1} kanamycin), as described in [15]. Decimal reduction rate from plate count measurements was calculated as: $N = log\left(\frac{Gen^R\,cells}{Gen^R Kan^r\,cells}\right)$.

2.3.4. Flow cytometry

Cell permeability (propidium iodide staining/FL3 channel) and the eGFP-fluorescence of plasmid-expressing cells (FL1 channel) were measured by the BD Accuri C6® flow cytometer (BD Biosciences, Franklin Lakes, NJ, USA). Cell samples were diluted in physiological solution at 10^6 cells·ml^{-1} and then, were stained with 20 μl of a commercial solution of propidium iodide at 20 mg l^{-1} (*abbr.* PI) (Molecular Probes, Invitrogen, USA) and incubated 20 min at room temperature in the dark. A 100 % dead–cell control was prepared by incubating cells in 70 % isopropanol for 1 h at room temperature. Samples were run until 20, 000 events were counted at 14 μl min^{-1} using milli-Q water as sheath fluid. The Forward Scatter Signal (threshold: 12, 000) and Side Scatter Signal (threshold: 2, 000) were used as trigger channels. Data acquisition was performed with BD Accuri CFlow® software and data processing was achieved with FlowJo software (Becton Dickinson, Sparks, MD, USA). Decimal reduction rate was calculated as described above from plasmid-expressing cells (eGFP-positive cells, FL1-A > $8{\cdot}10^2$) and total cells (Single cells, bisectors of both FCS-A *vs* FSC-H and SSC-A *vs* SSC-H): $N = log\left(\frac{Single-cells}{eGFP-cells}\right)$.

2.3.5. Fluorescence measurement in the medium

Extracellular fluorescence intensity in the supernatant was measured using a multiplate reader as described in [15]. Relative extracellular fluorescence intensity was calculated as: $RFU = \frac{FU_t - FU_{t_0}}{OD_t - OD_{t_0}}$. The optical density considered was corrected with the percentage of intact cells (*i.e.* not stained by propidium iodide).

2.4. Data analysis

Specific substrate consumption (fructose q_S, ammonium q_N) and biomass production (μ) rates were calculated from experimental data and mass balances (carbon, nitrogen and elemental). Specific growth rate was determined as $ln\left(Xg_{CDW} \bullet l^{-1}\right) = f(t)$ and its error was calculated as the standard deviation of the slope. Determination of specific oxygen consumption (q_{O_2}) and carbon dioxide production (q_{CO_2}) was based on mass balance calculations in both liquid and gaseous phase, from inlet/outlet gas composition, temperature, pH, stirring, oxygen partial pressure (pO_2), and liquid volume. For overall production/consumption yield calculation, masses were plotted pairwise in a scatter plot. A linear regression was used to determine the considered yields and the error was calculated by the standard deviation of the slope. The total mass of isopropanol and acetone produced were calculated by summing the masses of solvents in the bioreactor (liquid phase) and in the two guard flasks (evaporation).

2.4.1. Statistical analysis: normality of distribution functions by BoxPlot representation

Boxplot representation used to represent fluorescence intensity distribution in single cells was described in Boy et al. (2020).

3. Results

The behavior of the strain Re2133/pJLCB2, engineered to constitutively express eGFP protein and synthesize isopropanol after arabinose induction, was compared to the Re2133/pCB1 fluorescent strain and the Re2133/pEG7c isopropanol over-producer. The characterization of the strains was achieved during fed-batch cultivation where fructose was fed continuously as the sole carbon source under controlled nitrogen limitation.

3.1. Growth kinetics and isopropanol production

During batch phases, the maximum growth rates were close for the three strains, with 0.23 ± 0.02 h^{-1} for Re2133/pEG7c (isopropanol operon), 0.21 ± 0.03 h^{-1} for Re2133/pJLCB2 (isopropanol operon + *egfp* cassette) and 0.24 ± 0.01 h^{-1} for Re2133/pCB1 (*egfp* cassette) (Table 2 & Fig. 1b). During nitrogen limited fed-batch, after arabinose induction, Re2133/pEG7c and Re2133/pJLCB2 began to produce isopropanol. Growth rates were maintained at a controlled growth rate of 0.03 ± 0.01 h^{-1} for Re2133/pEG7c, 0.04 ± 0.01 h^{-1} for pJLCB2 and 0.04 ± 0.01 h^{-1} for pCB1 by controlled nitrogen limitation (Fig. 1b).

Substrate consumption and metabolite production were quantified. In all cases, the carbon, nitrogen and elemental balances were satisfied above 90 %. In fed-batch mode, the maximum isopropanol concentration reached was 5.3 g l^{-1} (38 h after induction) for the strain Re2133/pJLCB2 and 15.1 g l^{-1} (76 h after induction) for Re2133/pEG7c (Table 2). Isopropanol was produced at a maximum production yield of 0.27 ± 0.01 $g_{IPA}{\cdot}g_S^{-1}$ for Re2133/pEG7c and 0.11 ± 0.02 $g_{IPA}{\cdot}g_S^{-1}$ for Re2133/pJLCB2, at the start of the fed-batch phase, before decreasing for all the strains (Table 2). Profiles of isopropanol specific production rates showed the same dynamics for both strains (Fig. 1e). First, after arabinose induction, the specific isopropanol production rate increased up to a maximum, which was equal to 0.09 $g_{IPA}{\cdot}g_S^{-1}{\cdot}h^{-1}$ (30 h) for Re2133/pEG7c, and 0.04 $g_{IPA}{\cdot}g_S^{-1}{\cdot}h^{-1}$ (20 h) for pJLCB2, before decreasing. The maximum isopropanol yield was reached over this period of time. Then, the specific production rate of isopropanol was low until the end of the culture.

Acetone is an intermediate in the isopropanol production pathway. It was produced simultaneously with isopropanol throughout the fed-batch cultures (Fig. 1 d & e). The maximum yields of acetone production from fructose reached 0.024 ± 0.001 $g_{Ac}{\cdot}g_S^{-1}$ for Re2133/pEG7c and 0.011 ± 0.001 $g_{Ac}{\cdot}g_S^{-1}$ for pJLCB2 respectively (Table 2). The profiles of the specific acetone production rate followed the same behavior as for those of isopropanol, confirming that the two productions were coupled. The maximal acetone production rates were 0.009 $g_{Ac}{\cdot}g_S^{-1}{\cdot}h^{-1}$ for Re2133/pEG7c and 0.002 $g_{Ac}{\cdot}g_S^{-1}{\cdot}h^{-1}$ for pJLCB2 (Fig. 1e).

No significant organic acid production was detected during cultivation for any of the strains. However, after induction by arabinose, a slight peak in pyruvic acid production was observed for the strain Re2133/pEG7c but was re-consumed shortly afterwards; this was not

Table 2
Fed-batch cultivation parameters of the strains Re2133/pEG7c, pJLCB2 and pCB1. N/A; not applicable.

	μ_{max} (h^{-1})	μ_{prod} (h^{-1})	$[isopropanol]_{max}$ ($g\ L^{-1}$)	Yield biomass ($g\ g^{-1}$)	Yield CO_2 ($g\ g^{-1}$)	Yield isopropanol ($g\ g^{-1}$)	Yield acetone ($g\ g^{-1}$)	$[isopropanol]_{Critical}$ ($g\ L^{-1}$)
pEG7c	0.23 ± 0.02	0.03 ± 0.01	15.1	0.44 ± 0.02 (batch) 0.09 ± 0.01 (19–35 h) 0.17 ± 0.01 (47–92 h)	0.54 ± 0.03 (batch) 0.65 ± 0.01 (19–35 h) 0.90 ± 0.01 (47–92 h)	**0.27 ± 0.01** (19–35 h) 0.098 ± 0.003 (47–92 h)	**0.024 ± 0.001** (19–35 h) 0.007 ± 0.003 (47–92 h)	15.1
pJLCB2	0.21 ± 0.03	0.04 ± 0.01	5.3	0.48 ± 0.04 (batch) 0.19 ± 0.01 (14–45 h) 0.30 ± 0.001 (48–77 h)	0.66 ± 0.04 (batch) 0.62 ± 0.01 (14–45 h) 0.86 ± 0.01 (48–77 h)	**0.11 ± 0.01** (14–45 h) 0.004 ± 0.001 (48–77 h)	**0.011 ± 0.001** (14–45 h) 0.006 ± 0.001 (48–77 h)	5.3
pCB1	0.24 ± 0.01	0.04 ± 0.01	N/A	0.32 ± 0.01	0.89 ± 0.02	**N/A**	**N/A**	N/A

the case for Re2133/pCB1 or pJLCB2 as no pyruvate was detected at all.

Oxygen and carbon dioxide consumption rates were calculated from off gas analysis allowing the calculation of the respiratory quotient (*abbr.* RQ) (Fig. 1c). The respiratory quotient reached a maximum value a few hours after arabinose induction (Fig. 1c), at 1.96 (30 h) for pEG7c and 1.90 (29 h) for pJLCB2, approaching the theoretical value for isopropanol alone (= 1.96). For the strain Re2133/pCB1 it remained stable around 1.05 ± 0.06 in the range of the theoretical RQ for growth (= 1.06), before decreasing in the last hours of culture. For Re2133/pEG7c and pJLCB2, its value stabilized until the end of culture at respectively 1.30 ± 0.07 and 1.19 ± 0.06.

It was interesting to consider the variation in the ratio between isopropanol and acetone production (Fig. 1d). For the reference strain Re2133/pEG7c, this ratio remained stable at 13 ± 1 $Cmol_{IPA}/Cmol_{AC}$ from arabinose induction until the stop of isopropanol production. For the strain Re2133/pJLCB2, the evolution of this ratio was drastically different. Just after arabinose induction, its value reached 13 ± 1 $Cmol_{IPAl}/Cmol_{AC}$ which was equal to the behavior in Re2133/pEG7c. However, this value decreased continuously throughout the fermentation until it reached 4 $Cmol_{IPA}/Cmol_{AC}$ at the end of the culture. This meant that there was an accumulation of acetone to the detriment of the production of isopropanol at the end of the culture.

During the batch phase (Fig. 2), the distribution of carbon between biomass and carbon dioxide was comparable for the 3 strains Re2133/pEG7c (60: 40 %) pJLCB2 (62: 38 %) and pCB1 (65: 35 %). During the fedbatch, the strain Re2133/pJLCB2 has an intermediate proportion of biomass and CO_2 (28–50 %) comparing to strains Re2133/pEG7C (11–44 %) and Re2133/pCB1 (40–60 %). The highest isopropanol production yield was achieved when the specific isopropanol production rate was the highest for all strains. The percentage of the carbon flow dedicated to isopropanol reached 41 % for Re2133/pEG7c and 20 % for pJLCB2; the proportions of isopropanol and acetone were halved in Re2133/pJLCB2. The lower proportion of isopropanol in Re2133/pJLCB2 compared to pEG7c was mainly due to a higher carbon flow toward the biomass/eGFP synthesis (+ 17 %), and carbon dioxide (+ 6 %) to a lesser extent.

3.2. Inhibition by isopropanol production

After induction, the specific isopropanol production rate increased to a maximum ($q_{IPA,\ max}$) at a concentration of 1.4 g l^{-1} isopropanol produced for Re2133/pEG7c, and 0.4 g l^{-1} for pJLCB2 (Fig. 1e). For Re2133/pEG7c, the specific isopropanol production rate decreased (- 96 %) until 7.5 g l^{-1} of isopropanol were produced, then remained low and constant until it became null at 15.1 g l^{-1} of isopropanol. For Re2133/pJLCB2, the specific isopropanol specific production rate decreased until 5.3 g l^{-1} of isopropanol were produced, and became zero. For Re2133/pJLCB2, even when isopropanol concentration decreased in the medium due to higher amounts evaporated compared to the amounts produced, the specific isopropanol production rate remained zero. Thus, the critical isopropanol concentrations were equal to 15.1 g l^{-1} for Re2133/pEG7c and 5.3 g l^{-1} for pJLCB2. Same profiles were obtained regarding acetone production with almost 10 times lower specific production rates and critical acetone concentration values around 1 g.l^{-1} for both strains.

3.3. Plasmid expression levels variations during isopropanol production

Plasmid expression levels *via* single-cell eGFP fluorescence intensity monitoring were studied throughout the fermentation, with and without isopropanol production (strain Re2133/pJLCB2 *versus* strain Re2133/pCB1). Flow cytometry has been used as a fast and reliable method for fluorescence intensity measurements in single-cells (*i.e.* eGFP and PI). Plasmid stability was also assessed by the standard plate count method. The strains Re2133/pEG7c and pCB1 were used as reference, respectively for the production of isopropanol only and the single-cell fluorescence eGFP only, and compared to the strain Re2133/pJLCB2.

3.3.1. Plasmid expression levels analysis

The distribution of fluorescence intensity among single cells was studied for the strains Re2133/pCB1 and pJLCB2, with a boxplot representation (Fig. 3). The first observation was that fluorescence intensity in single cells was higher for Re2133/pJLCB2 than for Re2133/pCB1 during the batch phase. To solve a construction issue, the fluorescent cassette P_{lac}-*eGFP* had to be inserted on the opposite strand of DNA in pJLCB2, compared to the localization in the plasmid pCB1. Indeed, during the construction of the plasmid it appeared that there was an incompatibility for the fluorescent cassette and isopropanol operon to be localized on the same DNA strand. No convincing explanation for this phenomenon has yet been found. Higher fluorescent intensity of single cells for Re2133/pJLCB2 compared to pCB1 might be due to a higher induction of the promoter P_{lac} when located on the opposite DNA strand. Nevertheless, the threshold between fluorescent and non-fluorescent cells was still reached at 8.10^2 in the FL1-A channel for both strains.

For the strain Re2133/pCB1, the fluorescence intensity distribution of the total cell population was noisier during the first 30 h after nitrogen limitation (20–50 h) (Fig. 3a). During batch phase and after 60 h in fed-batch, fluorescence intensity distribution was considered close to Gaussian and reproducible over time. For the specific eGFP-positive cell population (Fig. 3c), the fluorescence intensity distribution was Gaussian and reproducible throughout the culture.

For the strain Re2133/pJLCB2, the fluorescence intensity distribution was Gaussian and reproducible throughout the batch phase, for total (Fig. 3b) and eGFP-positive cell populations (Fig. 3d). After arabinose induction, the median fell rapidly for the total cell population (Fig. 3b), the distribution interval increased drastically between 30 and

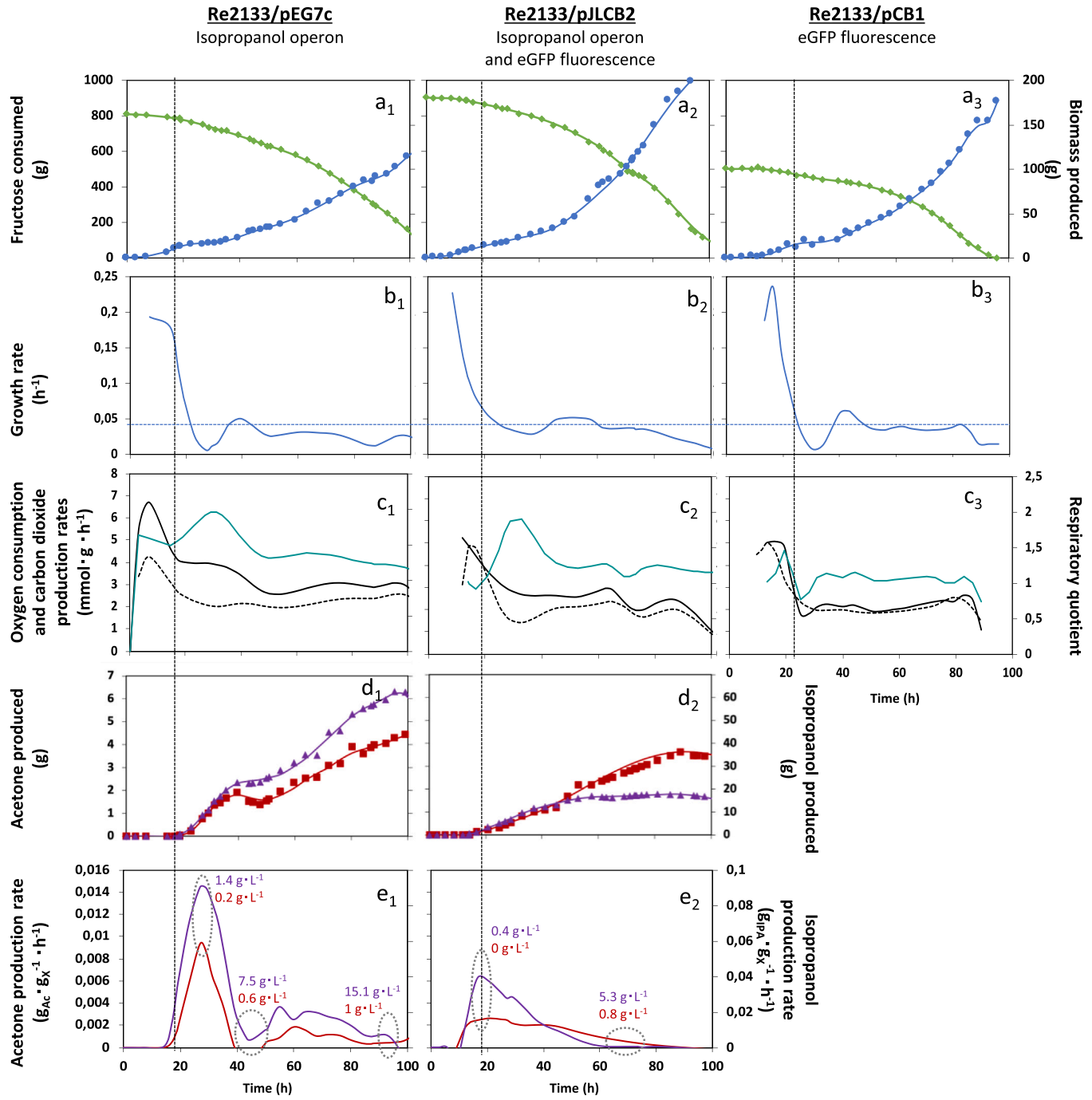

Fig. 1. (a). Cumulated biomass produced (●) and fructose consumed (◆). (b). Growth rate evolution through time (▰). (c). oxygen consumption (▰ ▰) and carbon dioxide (▰) production rates, and respiratory quotient (▰). (d). Cumulated acetone (■) and isopropanol (▲) produced during fed-batch. Evolution of isopropanol (▰) and acetone (▰) production rates. Cultures in fed-batch of the strains Re2133/pEG7c (1), pJLCB2 (2) and pCB1 (3). The horizontal dotted black line represented the time limit between the batch phase and the fed-batch phase. The doted circles (e1 & 2) represent the moments when specific production rate was either maximum or minimum, and the corresponding isopropanol/acetone concentrations reached.

40 h, and then more slowly until the end of the culture. After 30 h, the distribution could no longer be considered Gaussian. For the eGFP-positive cell population, the distribution range increased significantly between 30 and 40 h and then, remained stable (Fig. 3d). After that, the fluorescence intensity distribution was reproducible. The median and mean values slightly decreased and the first quartile became longer than the third quartile, as the number of less fluorescent cells increased.

3.4. *Plasmid expression stability: flow cytometry versus plate count*

The decimal reduction rate (Fig. 4) was used to compare the stability of plasmid expression by two reporters: eGFP biosensor (flow cytometry) and kanamycin resistance (plate count).

For Re2133/pEG7c, up to 9 g l^{-1} isopropanol (and 0.6 g l^{-1} of acetone), the decimal reduction rate calculated from the plate count remained low below 0.5 (Fig. 4a, d & f). From 9–14 g l^{-1} of isopropanol, the decimal reduction rate was maintained at 0.7. After 14 g l^{-1} of isopropanol, the decimal reduction rate increased up to 1.6.

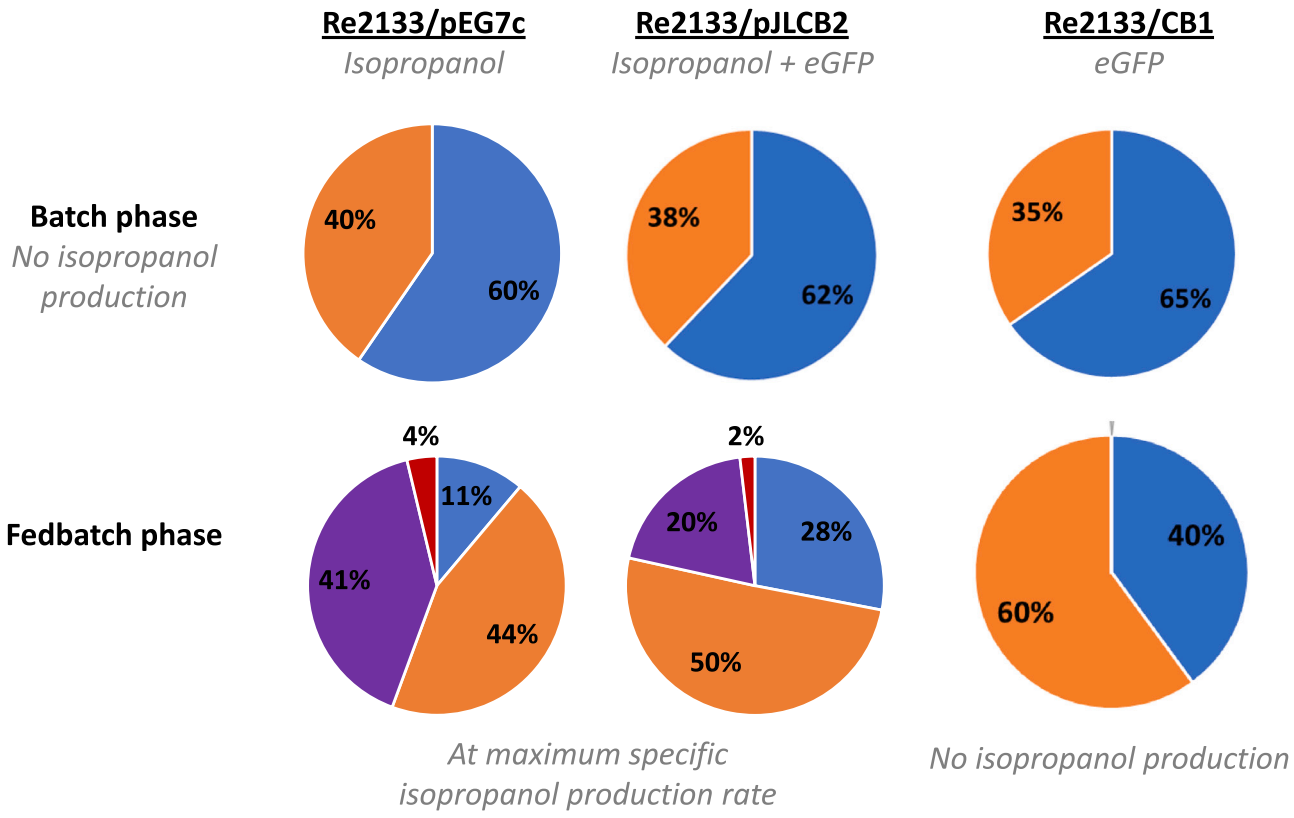

Fig. 2. Overall carbon repartition (% Cmol) between biomass (■), carbon dioxide (■), acetone (■) and isopropanol (■), based on global yields during culture of Re2133/pEG7c, pJLCB2 and pCB1.

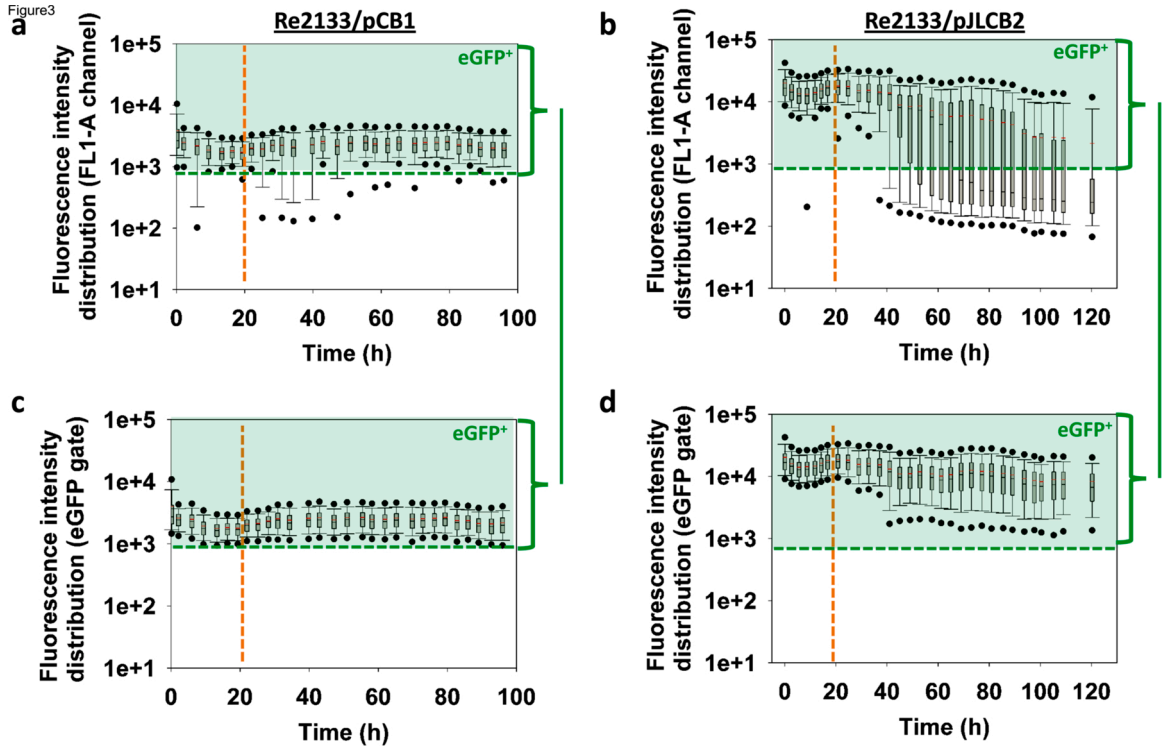

Fig. 3. Boxplot representation through time of fluorescence intensity distribution in the FL1-A channel for the total cell population of Re2133/pCB1 (a) and pJLCB2 (b), and for the eGFP-positive population of Re2133/pCB1 (c) and pJLCB2 (d). The vertical dotted orange line represented the limit between the batch and fed-batch phases and the horizontal dotted green line represented the eGFP-positive gate.

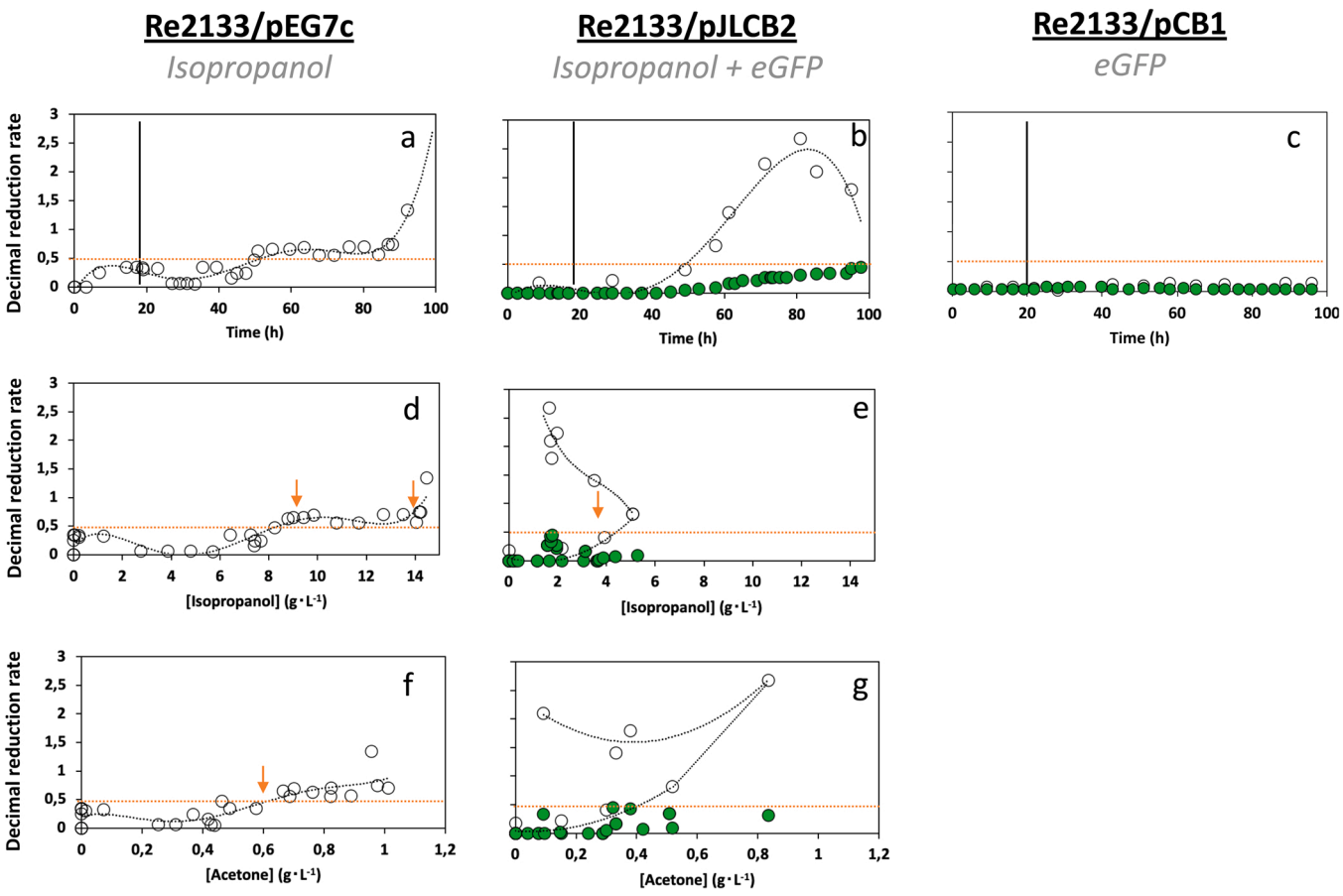

Fig. 4. Decimal reduction rate for the strains Re2133/pEG7c, pJLCB2 and pCB1 through time isopropanol and acetone concentrations, by plate count (•) and flow cytometry (●). The vertical black line represented the time limit between the batch phase and the fed-batch phase. Orange horizontal dotted lines represented the limit of a low decimal reduction level and orange arrows marked when this limit was crossed.

For Re2133/pJLCB2, the decimal reduction rate measured by plate counting was significantly higher than that measured by flow cytometry (Fig. 4b, e & g) and it began to increase once 3.6 g l^{-1} of isopropanol were produced in the liquid phase (21 h after induction, corresponding to 0.5 g l^{-1} of acetone). After 5.3 g l^{-1} of isopropanol produced in the liquid phase, the quantity of isopropanol evaporated was greater than the quantity of isopropanol produced in the liquid phase, therefore the isopropanol concentration in the liquid phase decreased. However, the decimal reduction rate calculated by plate count kept on increasing until reaching 2.6, value reached at a concentration as low as 1.7 g l^{-1} of isopropanol in the medium, because on this time period, acetone concentration had kept on increasing up to 0.8 g l^{-1}. After that point, the decimal reduction rate by plate count decreased slightly down to 1.5, as acetone concentration in the medium decreased as well, because of enhanced evaporation at the expense of production. When calculated from flow cytometry data, the decimal reduction rate remained low, even if a slight heterogeneity was measured around 2 g l^{-1} of isopropanol. For Re2133/pCB1, the decimal reduction rate was low throughout culture, for both counting methods (Fig. 4c).

It appeared that the plasmid stability was more affected by the overproduction of isopropanol than the production of recombinant protein e-GFP even if the decimal reduction rate for the single-construct remained at a low level. However, cumulative production of isopropanol and e-GFP protein was detrimental for the stability of plasmid-expression.

3.5. Cell permeability and eGFP leakage

To study the impact of isopropanol production and/or eGFP expression on cell physiology, permeability and extracellular fluorescence were studied during culture.

During the batch phase, all the strains showed a percentage of permeabilized close to zero (Fig. 5). For the strain Re2133/pEG7c, the percentage of permeabilization remained low (<5 %) up to 55 h of culture, corresponding to 9 g l^{-1} of isopropanol and 0.6 g l^{-1} acetone (Fig. 5a & d). Then, it increased gradually until it reached 25 % at the end of the culture. For the strain Re2133/pCB1, a slight transient peak at 8 % was measured just after the beginning of the fed-batch phase (Fig. 5c). This was due to a nitrogen depletion phase that was longer (3 h) for this strain compared to Re2133/pEG7c and pJLCB2 (less than 1 h), due to technical problems at the initiation of nitrogen feeding. Then, cell permeabilization percentage maintained low, under 5 %, all along fermentation. For Re2133/pJLCB2, contrary to strain Re2133/pEG7c, cell permeability increased as soon as isopropanol and acetone started to accumulate in the medium (Fig. 5b & e). Even though, the concentration of isopropanol and acetone remained below 6 g. l^{-1} and 0.8 g l^{-1}, respectively, cell permeabilization increased continuously to reach 25 % at the end of culture. For the same concentration of isopropanol produced, cell permeabilization percentage was much lower for Re2133/pEG7c than for pJLCB2. The strain Re2133/pJLCB2 appears clearly less tolerant to acetone and/or isopropanol than Re2133/pEG7c.

Relative extracellular fluorescence intensity in the supernatant was largely higher for Re2133/pJLCB2 than for Re2133/pCB1 all along the culture (Fig. 5b, e & d). This was consistent with the fact that the permeabilization percentage was significantly higher for Re2133/pJLCB2 all along the culture and that the fluorescence intensity of single-cells was higher in Re2133/pJLCB2 than in Re2133/pCB1.

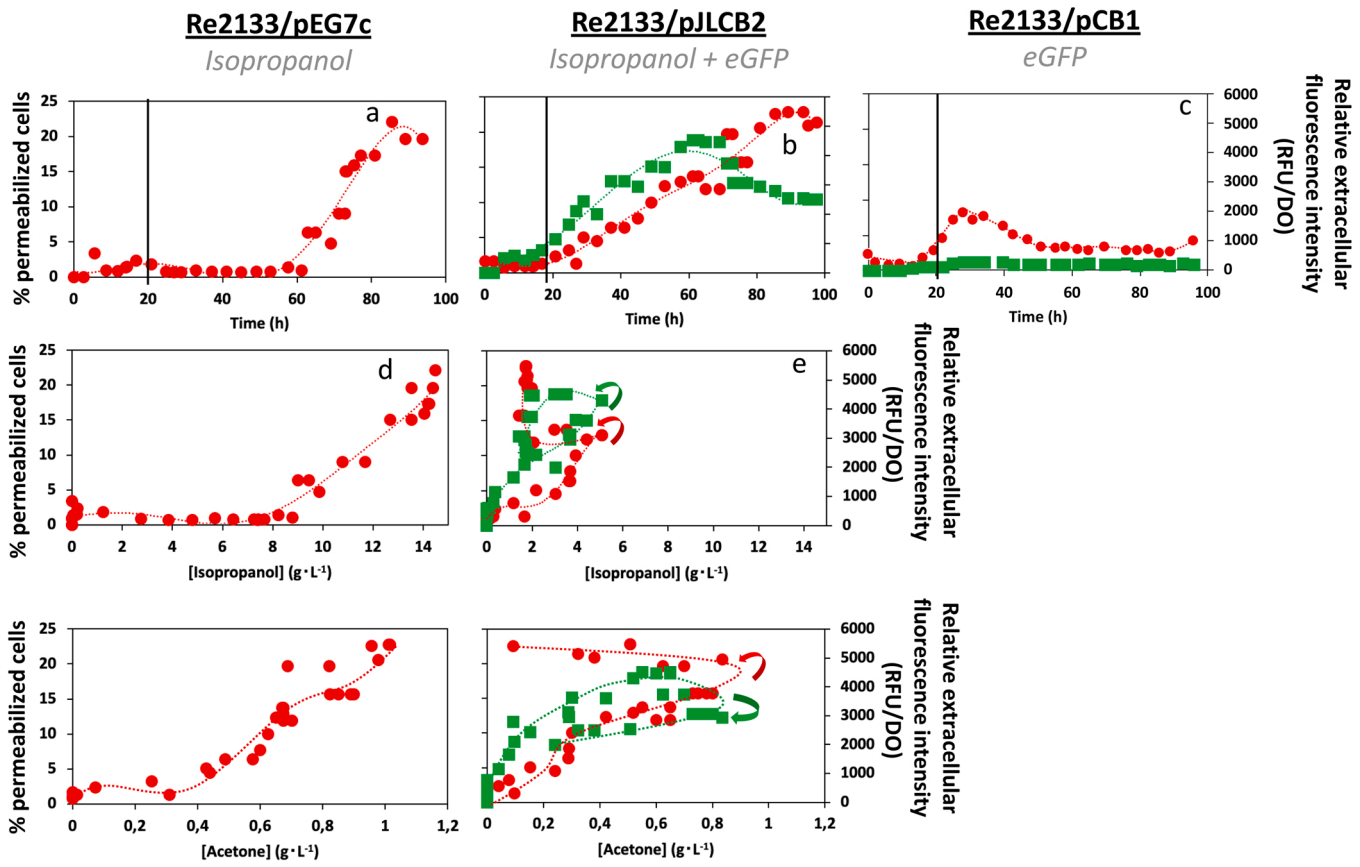

Fig. 5. Cell permeabilization percentage (●) for the strains Re2133/pEG7c, pJLCB2 and pCB1 *vs* time, isopropanol and acetone concentrations and Relative extracellular fluorescence intensity (■) for Re2133/pJLCB2 and pCB1. The horizontal dotted black line represented the time limit between the batch phase and the fed-batch phase.

4. Discussion

A plasmid-encoded biosensor was used to monitor and quantify variations in plasmid expression levels at the single cell level. This study was carried out in the particular case of isopropanol production from fructose by *C. necator*. The isopropanol production pathway was plasmid-encoded as well. The objective of this work was to study the impact of isopropanol and eGFP productions on plasmid expression levels and isopropanol production.

The maximum titer of isopropanol produced was much higher for the reference strain Re2133/pEG7c (15.1 g l^{-1}) compared to Re2133/pJLCB2 (5.3 g l^{-1}, - 65 %). In addition, a higher maximum isopropanol production yield was measured for Re2133/pEG7c (+ 59 %) compared to Re2133/pJLCB2. Thus, the maximum production yield depended on whether or not eGFP was expressed.

When the isopropanol concentration increased for Re2133/pEG7c and pJLCB2, the membrane permeability increased up to 25 %, compared to Re2133/pCB1, the non-isopropanol producing strain (<5 %). Indeed, cell permeability and membrane fluidity have been shown to increase in response to higher alcohol concentration in producing strains [51]. The strain Re2133/pEG7c showed a better tolerance toward isopropanol and acetone in terms of cell permeability (<5 % up to 8 g l^{-1} isopropanol and 0.5 g l^{-1} acetone) compared to Re2133/pJLCB2 (<5 % up to 2 g l^{-1} isopropanol and 0.2 g l^{-1} acetone). This could be explained by the fact that Re2133/pJLCB2 also produced eGFP. Depending on culture conditions, GFP has been shown to increase cell permeability [52]. Under optimal growth conditions, cell permeability in fluorescent cells remained low as obtained with the strain Re2133/pCB1. However, under more challenging culture conditions, such as isopropanol production or fluctuating environments [20], eGFP might contribute increase cell permeability.

As cell permeability increased during isopropanol production, eGFP leaked outside the cells during fed-batch cultivation. Indeed, the relative intensity of the extracellular fluorescence increased gradually until the critical concentrations of isopropanol and acetone (5.3 and 0.8 g l^{-1} respectively) were reached in the medium for Re2133/pJLCB2 (60 h). Both isopropanol and acetone have shown a negative impact on cell permeability. Acetone could have a greater impact on cell permeability being a more hydrophobic solvent, which could solubilize the phospholipidic membrane of cells [47–49]. On the contrary, the relative extracellular intensity for the strain Re2133/pCB1 was insignificant compared to Re2133/pJLCB2. This could be due to two phenomena: i) higher intracellular fluorescence intensity of single-cells for Re213/pJLCB2 due to strain construction and ii) higher cell permeability for this strain. These statements could be supported by the distribution of fluorescence intensity within the population which decreased over the same period. Thus, monitoring of plasmid expression levels *via* biosensor was biased by intracellular fluorescence leakage due to increased permeability. However, this sensor made it possible to highlight the potential loss of intracellular compounds (proteins, nucleic acids, co-factors, etc.) that the strain would have to manage under production of an unnatural toxic molecule, such as isopropanol. Such a loss would certainly have an impact on the strain and therefore on the robustness of the process.

For Re2133/pJLCB2, the rate of decimal reduction (*i.e.* loss of plasmid expression) started to increase as revealed by two counting methods (plate count and flow cytometry) when a concentration of 3.6 g l^{-1} of isopropanol was reached in the bioreactor (60 h), which was close to the critical isopropanol concentration (5.3 g l^{-1}). As the isopropanol concentration decreased, the decimal reduction rate increased further in

response to increasing acetone concentrations. Subsequently, the decimal reduction rate increased drastically to 2.6 by plate count and to 0.5 by flow cytometry. Thus, for Re2133/pJLCB2, isopropanol and acetone were observed to have a negative impact on the stability of plasmid expression. A similar behavior could be observed for Re2133/pEG7c, but to a lesser extent. The additional increase in the rate of decimal reduction by plate count (compared to flow cytometry) was due to the decrease in cell cultivability itself due to increased isopropanol concentrations [46] When no isopropanol/acetone was produced, the decimal reduction rate was low throughout culture for Re2133/pCB1. Thus the decimal reduction rate by plate count reflects both cell cultivability and plasmid expression stability, which were both lower for Re2133/pJLCB2 compared to pEG7c and pCB1. In contrast, the decimal reduction rate by flow cytometry only reflects the stability of plasmid expression, which was lower for Re2133/pJLCB2 compared to pCB1. Thus, the decrease in the decimal reduction rate measured by plate count at the end of the culture with Re2133/pJLCB2 could be due to the decrease in isopropanol concentration (*i.e.* evaporation > production) in the medium and therefore to a lower toxicity of the environment. Therefore, new-forming cells were subjected to lower isopropanol concentrations and exhibited better cultivability, which reduced the gap between the two counting methods. This could explain why the decimal reduction rate by flow cytometry continuously increased over the same period, since it was not affected by cell cultivability. Thus, isopropanol and acetone productions have a negative impact on both cell cultivability and plasmid expression stability. Moreover, the production of isopropanol and eGFP by strain Re2133/pJLCB2 caused an increase in the loss of plasmid expression and cell cultivability compared to pCB1 and pEG7c. Finally, a decrease in the stability of plasmid expression appeared to cause a decrease in the specific production rate of isopropanol. As plasmid expression was destabilized earlier for Re2133/pJLCB2, it was consistent with the strain's lower isopropanol production performance.

As plasmid expression stability was lower for strain Re2133/pJLCB2, a higher proportion of the carbon flow was dedicated to CO_2 and biomass production (50 % and 28 % respectively at $q_{IPA,\ max}$), compared to strain Re2133/pEG7c (44 % and 11 %, respectively at $q_{IPA,\ max}$). Therefore, carbon flux toward acetone (2 % at $q_{IPA,\ max}$) and isopropanol (20 % at $q_{IPA,\ max}$) was strongly decreased for this strain (4 % and 44 % respectively, for pEG7c at $q_{IPA,\ max}$). To overcome this phenomenon, it could be beneficial to reduce the production growth rate in order to favor the isopropanol production.

Now, given the distribution of carbon between isopropanol and acetone, acetone accumulated in the medium in higher proportions for strain Re2133/pJLCB2 compared to pEG7c, to the detriment of the isopropanol biosynthesis. This less efficient carbon redirection to isopropanol could be caused by lower specific activity of ADH (*i.e.* alcohol dehydrogenase) compared to ADC (*i.e.* acetoacetate decarboxylase), leading to a bottleneck in the hydrogenation of acetone and thus to the accumulation of acetone. It could also be due to a lower availability of NADPH, H^+ for the hydrogenation of acetone [40].

Marc and coworkers (2017) showed that an enhancement of the specific activity of heterologous enzymes of the isopropanol synthesis pathway (*i.e.* ADC, ADH) *via* the expression of chaperones contributed to improved cellular tolerance to isopropanol and led to better carbon redirection to isopropanol. Indeed, with increasing isopropanol concentrations, intracellular proteins are likely to be partially or completely denatured [53]. This could disrupt the activity of enzymes as well as transcription and translation. As we have shown that fluorescence expression in Re2133/pJLCB2 increased permeability upon isopropanol production, it could be advantageous to add a chaperon protein expression system (*ex.* GroELS) on the plasmid in order to stabilize protein expression. Since eGFP was also produced in Re2133/pJLCB2 it might have disrupted enzyme expression by competing ribosomes, tRNA or amino acid availability compared to non-fluorescent strains [9]. However, at the isopropanol concentrations considered (maximum 15.1 g l^{-1}), the intrinsic fluorescence intensity of eGFP should not be significantly disrupted, since an isopropanol concentration of 235 g l^{-1} (30 % v/v) has already been successfully applied to purify eGFP by chromatography, without disrupting the fluorescence signal [54]. Thus, a change in the fluorescence intensity distributions was only due to a change in the amount of eGFP molecules present in the cells, and not to a change in the fluorescence signal of the eGFP molecules due to denaturation by isopropanol.

In conclusion, the heterogeneity of the plasmid expression level during the over-production of unnatural isopropanol by a fluorescent strain of *C. necator* cultured in fed-batch mode was evaluated by comparing the behavior at the single-cell and population levels of the 3 strains (isopropanol producer, eGFP producer, and isopropanol/eGFP co-producers). A link could be established between the variations of the fluorescence intensity distribution and the isopropanol/acetone production rates and titers. Thus, the use of the eGFP-reporter coupled to single cell analysis provided complementary information to the more traditional plate count method. However, isopropanol/eGFP co-expression had limitations especially in terms of isopropanol production. Indeed, the coupled productions of isopropanol and eGFP in Re2133/pJLCB2 led to enhance cell permeability compared to pEG7c. In addition, the plasmid stability was disrupted and resulted in decreased production rates of major metabolites, as the redirection of carbon flux to isopropanol synthesis was less efficient than in the reference strain. Thus, even if a complete understanding of the mechanisms leading to the heterogeneity of plasmid expression during isopropanol production has not yet been achieved, this work has made possible to highlight the increase in membrane permeability due to the isopropanol/acetone production most likely leading to loss of intracellular compounds and also to highlight the conflicting interactions between two different production pathway (*i.e.*) isopropanol and eGFP reporter system.

Compliance with ethical standards

N/A.

Ethical approval

Not applicable, since the work does not involve any study with human participants or animals.

Authors' contributions statement

CB, JL, SA, NG and SG conceived and designed research. CB conducted experiments and analyzed data. CB wrote the manuscript and JL, SA, NG and SG reviewed it. All authors read and approved the manuscript.

Declaration

N/A.

Funding

Funding was obtained from Doctoral Research Assignments from the French Ministry of Research.

Author agreement

All co-authors have approved this manuscript and accepted its submission. We confirm that none of the material in this manuscript has been previously published or is under consideration for publication elsewhere. The manuscript was not previously submitted to the journal "Enzyme and Microbial Technology". We certify there is no conflict of interest and that the manuscript is an original work of the authors.

Ethics approval

Not applicable, since the work does not involve any study with human participants or animals.

Consent to participate

Not applicable.

Consent for publication

All authors agreed to publish this work.

Data Availability

All data generated or analyzed during this study are included in the present work.

Code Availability

Not applicable.

Authors' contributions

CB, JL, SA, NG and SG conceived and designed research. CB conducted experiments and analyzed data. CB wrote the manuscript and JL, SA, NG and SG reviewed it. All authors read and approved the manuscript.

Supplementary Material 1

The plasmid maps of the plasmids pEG7c (arabinose induced isopropanol operon), pCB1 (constitutive Plac-eGFP) and pJLCB2 (combining the two genetic parts).

Competing interests

The authors declare that there are no competing interests.

Appendix A. Supporting information

Supplementary data associated with this article can be found in the online version at doi:10.1016/j.enzmictec.2022.110114.

References

[1] P.S. Swain, M.B. Elowitz, E.D. Siggia, Intrinsic and extrinsic contributions to stochasticity in gene expression, Proc. Natl. Acad. Sci. USA 99 (20) (2002) 12795–12800.

[2] H. Cao, O.P. Kuipers, Influence of global gene regulatory networks on single cell heterogeneity of green fluorescent protein production in Bacillus subtilis, Microb. Cell Fact. 17 (1) (2018) 134.

[3] B.F. Brehm-Stecher, E.A. Johnson, Single-cell microbiology: tools, technologies, and applications, Microbiol. Mol. Biol. Rev. 68 (3) (2004), 538-+.

[4] A.L. Heins, D. Weuster-Botz, Population heterogeneity in microbial bioprocesses: origin, analysis, mechanisms, and future perspectives, Bioprocess Biosyst. Eng. 41 (7) (2018) 889–916.

[5] F. Calabrese, I. Voloshynovska, F. Musat, M. Thullner, M. Schlömann, H. H. Richnow, J. Lambrecht, S. Müller, L.Y. Wick, N. Musat, H. Stryhanyuk, Quantitation and comparison of phenotypic heterogeneity among single cells of monoclonal microbial populations, Front. Microbiol. 10 (2019), 2814-2814.

[6] M.B. Elowitz, A.J. Levine, E.D. Siggia, P.S. Swain, Stochastic gene expression in a single cell, Science 297 (5584) (2002) 1183–1186.

[7] J. Mortier, W. Tadesse, S.K. Govers, A. Aertsen, Stress-induced protein aggregates shape population heterogeneity in bacteria, Curr. Genet. 65 (4) (2019) 865–869.

[8] G.Y.G. Nana, C. Ripoll, A. Cabin-Flaman, D. Gibouin, A. Delaune, L. Janniere, G. Grancher, G. Chagny, C. Loutelier-Bourhis, E. Lentzen, P. Grysan, J.N. Audinot, V. Norris, Division-based, growth rate diversity in bacteria, Front. Microbiol. 9 (2018).

[9] F. Ceroni, A. Boo, S. Furini, T.E. Gorochowski, O. Borkowski, Y.N. Ladak, A. R. Awan, C. Gilbert, G.B. Stan, T. Ellis, Burden-driven feedback control of gene expression, Nat. Methods 15 (5) (2018) 387.

[10] F. Silva, J.A. Queiroz, F.C. Domingues, Evaluating metabolic stress and plasmid stability in plasmid DNA production by Escherichia coli, Biotechnol. Adv. 30 (3) (2012) 691–708.

[11] D. Binder, T. Drepper, K.E. Jaeger, F. Delvigne, W. Wiechert, D. Kohlheyer, A. Grunberger, Homogenizing bacterial cell factories: analysis and engineering of phenotypic heterogeneity, Metab. Eng. 42 (2017) 145–156.

[12] F. Delvigne, P. Goffin, Microbial heterogeneity affects bioprocess robustness: dynamic single-cell analysis contributes to understanding of microbial populations, Biotechnol. J. 9 (1) (2014) 61–72.

[13] R. Gonzalez-Cabaleiro, A.M. Mitchell, W. Smith, A. Wipat, I.D. Ofiteru, Heterogeneity in pure microbial systems: experimental measurements and modeling, Front. Microbiol. 8 (2017).

[14] D. Longo, J. Hasty, Dynamics of single-cell gene expression, Mol. Syst. Biol. 2 (2006), 64-64.

[15] C. Boy, J. Lesage, S. Alfenore, N. Gorret, S.E. Guillouet, Plasmid expression level heterogeneity monitoring via heterologous eGFP production at the single-cell level in Cupriavidus necator, Appl. Microbiol. Biotechnol. (2020).

[16] M. Carlquist, R.L. Fernandes, S. Helmark, A.L. Heins, L. Lundin, S.J. Sorensen, K. V. Gernaey, A.E. Lantz, Physiological heterogeneities in microbial populations and implications for physical stress tolerance, Microb. Cell. Fact. 11 (2012).

[17] F. Delvigne, Q. Zune, A.R. Lara, W. Al-Soud, S.J. Sørensen, Metabolic variability in bioprocessing: implications of microbial phenotypic heterogeneity, Trends Biotechnol. 32 (12) (2014) 608–616.

[18] S. Muller, H. Harms, T. Bley, Origin and analysis of microbial population heterogeneity in bioprocesses, Curr. Opin. Biotechnol. 21 (1) (2010) 100–113.

[19] U. Zielenkiewicz, P. Ceglowski, Mechanisms of plasmid stable maintenance with special focus on plasmid addiction systems, Acta Biochim. Pol. 48 (4) (2001) 1003–1023.

[20] C. Boy, J. Lesage, S. Alfenore, S.E. Guillouet, N. Gorret, Investigation of the robustness of Cupriavidus necator engineered strains during fed-batch cultures, AMB Express 11 (1) (2021) 151.

[21] C. Boy, J. Lesage, S. Alfenore, S.E. Guillouet, N. Gorret, Study of plasmid-based expression level heterogeneity under plasmid-curing like conditions in Cupriavidus necator, J. Biotechnol. 345 (2022) 17–29.

[22] M. Utratna, C.P. O'Byrne, Using enhanced green fluorescent protein (EGFP) promoter fusions to study gene regulation at single cell and population levels, Methods Mol. Biol. 1157 (2014) 233–247.

[23] E. Wons, D. Koscielniak, M. Szadkowska, M. Sektas, Evaluation of GFP reporter utility for analysis of transcriptional slippage during gene expression, Microb. Cell Factor. 17 (1) (2018) 150.

[24] C. Argueta, K. Yuksek, M. Summers, Construction and use of GFP reporter vectors for analysis of cell-type-specific gene expression in Nostoc punctiforme, J. Microbiol. Methods 59 (2) (2004) 181–188.

[25] M.C. Blokpoel, R. O'Toole, M.J. Smeulders, H.D. Williams, Development and application of unstable GFP variants to kinetic studies of mycobacterial gene expression, J. Microbiol. Methods 54 (2) (2003) 203–211.

[26] J.A. Carroll, P.E. Stewart, P. Rosa, A.F. Elias, C.F. Garon, An enhanced GFP reporter system to monitor gene expression in Borrelia burgdorferi, Microbiology 149 (Pt 7) (2003) 1819–1828.

[27] J. Morschhäuser, S. Michel, J. Hacker, Expression of a chromosomally integrated, single-copy GFP gene in Candida albicans, and its use as a reporter of gene regulation, Mol. Gen. Genet. 257 (4) (1998) 412–420.

[28] C.F. Budde, S.L. Riedel, L.B. Willis, C. Rha, A.J. Sinskey, Production of Poly(3-Hydroxybutyrate-co-3-Hydroxyhexanoate) from Plant Oil by Engineered Ralstonia eutropha Strains, Appl. Environ. Microbiol. 77 (9) (2011) 2847–2854.

[29] C.G. Friedrich, B. Bowien, B. Friedrich, Formate and oxalate metabolism in Alcaligenes eutrophus, J. Gen. Microbiol. 115 (1979) 185–192.

[30] S. Grunwald, A. Mottet, E. Grousseau, J.K. Plassmeier, M.K. Popovic, J. L. Uribelarrea, N. Gorret, S.E. Guillouet, A. Sinskey, Kinetic and stoichiometric characterization of organoautotrophic growth of Ralstonia eutropha on formic acid in fed-batch and continuous cultures, Microb. Biotechnol. 8 (1) (2015) 155–163.

[31] B.F. Johnson, R.Y. Stanier, Dissimilation of aromatic compounds by Alcaligenes Eutrophus, J. Bacteriol. 107 (2) (1971) 468–475.

[32] J. Marc, E. Grousseau, E. Lombard, A.J. Sinskey, N. Gorret, S.E. Guillouet, Over expression of GroESL in Cupriavidus necator for heterotrophic and autotrophic isopropanol production, Metab. Eng. 42 (2017) 74–84.

[33] K. Tanaka, A. Ishizaki, T. Kanamaru, T. Kawano, Production of poly(D-3-hydroxybutyrate) from CO(2), H(2), and O(2) by high cell density autotrophic cultivation of Alcaligenes eutrophus, Biotechnol. Bioeng. 45 (3) (1995) 268–275.

[34] L. Crepin, E. Lombard, S.E. Guillouet, Metabolic engineering of Cupriavidus necator for heterotrophic and autotrophic alka(e)ne production, Metab. Eng. 37 (2016) 92–101.

[35] L. Garrigues, L. Maignien, E. Lombard, J. Singh, S.E. Guillouet, Isopropanol production from carbon dioxide in Cupriavidus necator in a pressurized bioreactor, New Biotech. 56 (2020) 16–20.

[36] A. Pohlmann, W.F. Fricke, F. Reinecke, B. Kusian, H. Liesegang, R. Cramm, T. Eitinger, C. Ewering, M. Potter, E. Schwartz, A. Strittmatter, I. Voss, G. Gottschalk, A. Steinbuchel, B. Friedrich, B. Bowien, Genome sequence of the bioplastic-producing "Knallgas" bacterium Ralstonia eutropha H16, Nat. Biotechnol. 24 (10) (2006) 1257–1262.

[37] H.W. Ryu, S.K. Hahn, Y.K. Chang, H.N. Chang, Production of poly(3-hydroxybutyrate) by high cell density fed-batch culture of Alcaligenes eutrophus with phospate limitation, Biotechnol. Bioeng. 55 (1) (1997) 28–32.

[38] M. Koller, A. Atlić, M. Dias, A. Reiterer, G. Braunegg, Microbial PHA production from waste raw materials, in: G.G.-Q. Chen (Ed.), Plastics from Bacteria: Natural

Functions and Applications, Springer Berlin Heidelberg, Berlin, Heidelberg, 2010, pp. 85–119.
[39] A. Sydow, A. Pannek, T. Krieg, I. Huth, S.E. Guillouet, D. Holtmann, Expanding the genetic tool box for Cupriavidus necator by a stabilized L-rhamnose inducible plasmid system, J. Biotechnol. 263 (2017) 1–10.
[40] E. Grousseau, J.N. Lu, N. Gorret, S.E. Guillouet, A.J. Sinskey, Isopropanol production with engineered Cupriavidus necator as bioproduction platform, Appl. Microbiol. Biotechnol. 98 (9) (2014) 4277–4290.
[41] W.B. Black, L. Zhang, C. Kamoku, J.C. Liao, H. Li, Rearrangement of coenzyme A-acylated carbon chain enables synthesis of isobutanol via a novel pathway in Ralstonia eutropha, ACS Synth. Biol. 7 (3) (2018) 794–800.
[42] C. Ewering, F. Heuser, J.K. Benolken, C. Bramer, A. Steinbuchel, Metabolic engineering of strains of Ralstonia eutropha and Pseudomonas putida for biotechnological production of 2-methylcitric acid, Metab. Eng. 8 (6) (2006) 587–602.
[43] T. Hoefel, E. Wittmann, L. Reinecke, D. Weuster-Botz, Reaction engineering studies for the production of 2-hydroxyisobutyric acid with recombinant Cupriavidus necator H 16, Appl. Microbiol. Biotechnol. 88 (2) (2010) 477–484.
[44] T. Krieg, A. Sydow, S. Faust, I. Huth, D. Holtmann, CO(2) to terpenes: autotrophic and electroautotrophic α-humulene production with Cupriavidus necator, Angew. Chem. (Int. Ed. Engl.) 57 (7) (2018) 1879–1882.
[45] J. Muller, D. MacEachran, H. Burd, N. Sathitsuksanoh, C.H. Bi, Y.C. Yeh, T.S. Lee, N.J. Hillson, S.R. Chhabra, S.W. Singer, H.R. Beller, Engineering of Ralstonia eutropha H16 for autotrophic and heterotrophic production of methyl ketones, Appl. Environ. Microbiol. 79 (14) (2013) 4433–4439.
[46] J. Chakravarty, C.J. Brigham, Solvent production by engineered Ralstonia eutropha: channeling carbon to biofuel, Appl. Microbiol. Biotechnol. 102 (12) (2018) 5021–5031.
[47] A. Mukhopadhyay, Tolerance engineering in bacteria for the production of advanced biofuels and chemicals, Trends Microbiol. 23 (8) (2015) 498–508.
[48] M.J. Dunlop, Engineering microbes for tolerance to next-generation biofuels, Biotechnol. Biofuels 4 (1) (2011) 32.
[49] S.A. Nicolaou, S.M. Gaida, E.T. Papoutsakis, A comparative view of metabolite and substrate stress and tolerance in microbial bioprocessing: from biofuels and chemicals, to biocatalysis and bioremediation, Metab. Eng. 12 (4) (2010) 307–331.
[50] J.N. Lu, C.J. Brigham, C. Rha, A.J. Sinskey, Characterization of an extracellular lipase and its chaperone from Ralstonia eutropha H16, Appl. Microbiol. Biotechnol. 97 (6) (2013) 2443–2454.
[51] K. Jia, Y. Zhang, Y. Li, Systematic engineering of microorganisms to improve alcohol tolerance, Eng. Life Sci. 10 (2010) 422–429.
[52] A.M. Ansari, A.K. Ahmed, A.E. Matsangos, F. Lay, L.J. Born, G. Marti, J. W. Harmon, Z. Sun, Cellular GFP toxicity and immunogenicity: potential confounders in in vivo cell tracking experiments, Stem Cell Rev. Rep. 12 (5) (2016) 553–559.
[53] L.O. Ingram, T.M. Buttke, Effects of alcohols on micro-organisms, Adv. Microb. Physiol. 25 (1984) 253–300.
[54] S.R. McRae, C.L. Brown, G.R. Bushell, Rapid purification of EGFP, EYFP, and ECFP with high yield and purity, Protein Expr. Purif. 41 (1) (2005) 121–127.
[55] C.F. Budde, S.L. Riedel, L.B. Willis, C. Rha, A.J. Sinskey, Production of Poly(3-Hydroxybutyrate-co-3-Hydroxyhexanoate) from plant oil by engineered ralstonia eutropha strains, Appl. Environ. Microbiol. 77 (9) (2011) 2847–2854.
[56] T. Fukui, M. Suzuki, T. Tsuge, S. Nakamura, Microbial synthesis of poly((R)-3-hydroxybutyrate-co-3-hydroxypropionate) from unrelated carbon sources by engineered Cupriavidus necator, Biomacromolecules 10 (4) (2009) 700–706.